JOURNAL OF MATERIALS SCIENCE 13 (1978) 639–646

Deformation mechanisms in oriented high density polyethylene

S. G. BURNAY
M. D. D., AERE, Harwell, UK
G. W. GROVES
Department of Metallurgy and Science of Materials, University of Oxford, UK

The deformation behaviour of single crystal texture HDPE has been examined in tension as a function of the orientation of the tensile axis with respect to the chain direction. Over most of the orientation range examined, it was found that slip processes parallel to the chain direction were the dominant modes of deformation. Fibrillar slip becomes relatively more important than chain slip as the strain increases and as θ_0, the initial value of the angle between the tensile axis and the chain direction, decreases. Lamellar slip was only observed over a limited range of orientations due to the high initiation stress required for the process. At low θ_0 values, lamellar separation accounted for a substantial part of the applied strain. Stress-induced martensitic transformation, which was observed in samples with $\theta_0 > 26°$, cannot account for an important fraction of the strain although the resolved shear stress required for the activation of the martensitic transformations is of the same order of magnitude as that required for chain slip.

1. Introduction

The subject of deformation mechanisms in oriented polymers has recently been reviewed by Bowden and Young [1]. Crystalline polymers can deform plastically by slip, twinning or martensitic transformation as well as by deformation of the amorphous phase. These processes have been studied most intensively for the case of high-density polyethylene (HDPE). In this material, chain slip has frequently been identified [2–5]. Chain slip can be defined as slip between molecules in the molecular direction occurring sufficiently homogeneously within crystalline lamellae to rotate the plane of the lamellar surface by shear. Chain slip is therefore detected by X-rays as a change in the angle between the lamellar normal and the molecular direction. Fibrillar slip has also been proposed as a slip process acting in the same direction as chain slip but occurring on a much coarser scale, possibly between pre-existing fibrillar stacks of lamellae, such that the orientation of the lamellar surface is not directly affected. Hinton *et al.* [4] in a study of HDPE pulled at angles in the range 40° to 62° to the orientation direction concluded that fibrillar and chain slip occurred, with fibrillar slip becoming more important at larger strains. In addition to these processes which both give rise macroscopically to a shear parallel to the molecular direction, there are three mechanisms giving rise to a shear on planes parallel to the molecular direction, but with a shear direction normal to the molecules. In oriented HDPE compressed normal to the chain direction (1 0 0) [0 1 0] slip has been identified [6]. Twinning on (1 1 0) has been observed in compressed HDPE [6] and in drawn single crystals [7]. A stress-induced martensitic transformation also occurs in both single crystals [7] and bulk oriented HDPE [6]. In addition to the mechanisms of deformation of crystalline material two modes of deformation within the amorphous phase have been observed. These are lamellar slip, and lamellar separation, both observed in double-textured HDPE pulled in a direction at 45° to the planes of the lamellae but nearly parallel to the molecular direction [5].

Although X-ray studies of deformed oriented HDPE have revealed various deformation mech-

anisms as indicated above, there is a lack of information on the change in relative importance of the mechanisms as the tensile stress direction is varied over a wide range of angles with respect to the molecular direction. Furthermore, most of the studies have been carried out without measurement of the stress required to produce the deformation, or that existing during the X-ray exposures. In this paper we report results obtained from single-crystal texture HDPE in which the tensile axis was varied in the (1 0 0) plane over the full range of angles for which ductile behaviour was observed, the tensile load being monitored during the deformation and subsequent X-ray exposures by a load cell attached to the straining jig. In this way we have built up a relatively complete picture of the plastic deformation in tension over a wide range of orientations.

2. Experimental

Sheets of HDPE 10 mm thick were compression-moulded from Rigidex 2 granules and blocks cut from the sheet were oriented by plane strain compression at 120° C, using a technique similar to that reported by Young *et al.* [2]. After compression-orienting, the samples were annealed at 126° C, lightly clamped to prevent warping. This differed from the procedure of Young *et al.* [2], who annealed at 207° C under 4 kbar pressure in order to remove monoclinic phases. In our case the monoclinic phase was not present after compression-orienting, and annealing at atmospheric pressure was found to produce a satisfactory single-crystal texture. The compression ratio chosen was a compromise between a high value giving a sharper texture but poor ductility and a low value giving a more diffuse texture but good ductility. A ratio of initial to final specimen thickness of 6.7 was finally chosen. The pole figure for this case is shown in Fig. 1; the texture is similar to although less sharp than that reported by Gray and Young [8]. It is worth recording that samples of Rigidex 9, the polymer used by Young *et al.* [2], were also prepared but were found to have substantially inferior tensile ductility for a given compression ratio than samples of Rigidex 2. This difference could not be attributed to a difference in the sharpness of crystallographic texture, which was found to be the same in Rigidex 9 and Rigidex 2 at a given compression ratio. The tensile deformation experiments were therefore carried out on Rigidex 2.

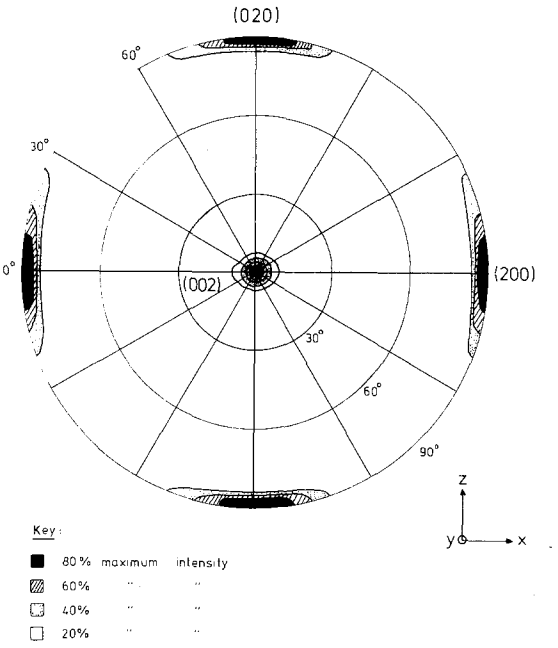

Figure 1 Pole figure for compression-oriented Rigidex 2 sample annealed 126° C (ratio of initial to final thickness = 6.7).

The compression-oriented and annealed sheet had a sufficient area, 800 mm^2, to allow tensile specimens to be cut out at different angles to the molecular direction in the (1 0 0) plane. The specimens had a gauge length of 3 mm and were 2 mm × 1.5 mm in cross-section. They were strained in a screw-driven jig for which a load cell was constructed, the jig being mounted on a Rigaku–Denki small-angle X-ray camera. The specimen strain at the position of the X-ray beam was measured from photographs of a gold grid evaporated onto the surface of the specimen. After a small angle X-ray pattern (SAX) was taken a wide angle pattern (WAX) was recorded on the same film by re-locating the film holder; an optical photograph of the specimen was recorded in the same position and on the same film through a simple pin-hole camera. This procedure reduced as far as possible the errors in measuring the angles between the wide angle reflections and the tensile axis of the specimen.

The specimens were strained in increments, then unloaded and allowed to relax after each strain increment; X-ray photographs were taken before and after removal of the load. While the specimens were being held at constant strain for the first X-ray exposure, some load relaxation occurred and this was recorded. The second X-ray exposure was taken with the load completely removed.

3. Interpretation of X-ray photographs

The analysis of the SAX and WAX patterns follows the lines of previous work [1–5]. The deformation is supposed in general to consist of a mixture of chain slip, fibrillar slip, lamellar slip and lamellar separation. This omits consideration of the transverse slip, twinning or martensitic transformation mechanisms. The justification for this lies in the observation that the strain component in the OZ direction (normal to the plane of the sheet and to the chain direction) is relatively small. Fig. 2 shows the measured ratios of the OY′ and OZ strains, OY′ being the direction normal to the tensile axis and to OZ. The operation of one of the transverse shear mechanisms would produce a contraction along OZ; these mechanisms become more favoured by the applied stress as θ, the angle between the tensile stress and the molecular direction, approaches 90°. However, the strain along OZ follows the opposite trend, becoming small as θ increases. The form of the strain is therefore inconsistent with transverse shear processes accounting for a substantial part of the total strain, though this does not rule out their occurrence to a small extent. The lamellar separation process may also be accompanied by some contraction along OZ but this is consistent with the observed strain since lamellar separation is the more favoured as θ approaches zero.

In the analysis, the amount of chain slip occurring can be deduced immediately. If the shear strain due to chain slip is γ_c, then

$$\gamma_c = \tan(\phi - \theta) \qquad (1)$$

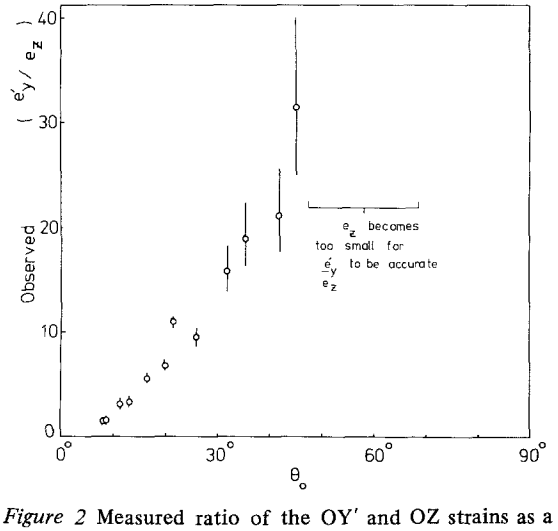

Figure 2 Measured ratio of the OY′ and OZ strains as a function of initial orientation θ_0.

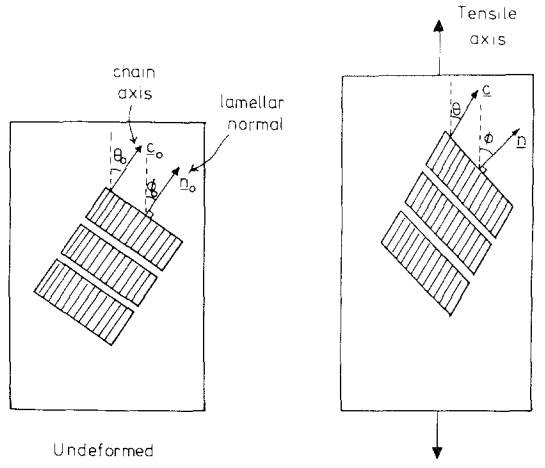

Figure 3 Schematic representation of chain slip.

where ϕ is the angle between the tensile axis and the lamellar normal and θ the angle between the tensile axis and the chain direction (Fig. 3). The lamellar separation in the tensile axis direction $\delta d/d$ can in principle be obtained directly from the SAX pattern although in practice the measurement, from the spacing of the small angle maxima, is often relatively inaccurate. The shears due to lamellar slip γ_L and fibrillar slip γ_F are more difficult to obtain. If an increment of specimen elongation $\delta h/h$ produces a change in θ of $\delta\theta$, the following equations [9] give the increments of lamellar slip and fibrillar slip;

$$\delta\gamma_L = \frac{(\delta h/h - \delta d/d) + \cot\theta\delta\theta}{\cot\theta\cos^2\phi + \cos\phi\sin\phi} \qquad (2)$$

$$\delta\gamma_F = \frac{(\delta h/h - \delta d/d) - \tan\phi\delta\theta}{\cos\theta\sin\theta + \tan\phi\sin^2\theta} - \delta\gamma_c \qquad (3)$$

4. Results and discussion

Specimens with initial angles between the tensile axis and the chain direction, θ_0, of 0°, 8°, 26°, 41° and 58° were tested (an attempt was also made to test at $\theta_0 = 75°$ and 90° but these specimens failed in a brittle manner). Over this range of orientation more than one deformation mechanism operates and the results will be summarized under the headings of the various mechanisms observed. Except at $\theta_0 = 0°$ and $\theta_0 = 8°$ the changes in θ and ϕ which occurred on unloading lay within the experimental error of angular measurement. The percentage of the macroscopic strain recovered upon unloading after a period of about 6 h was as high as 70% for $\theta_0 = 0°$ but for

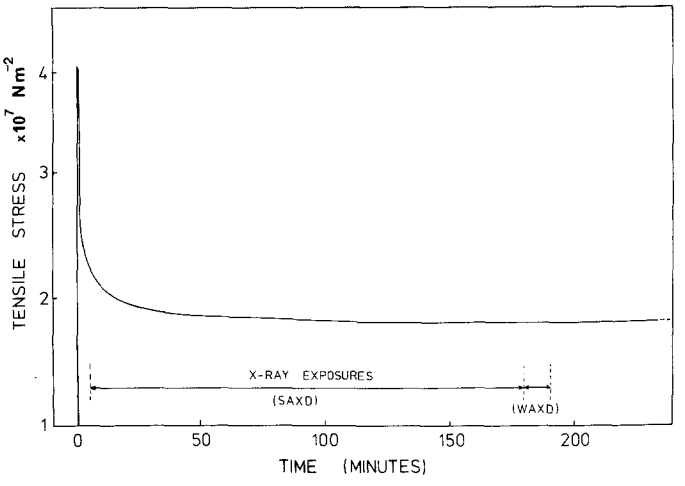

Figure 4 Typical stress relaxation curve following a strain increment.

the three highest values of θ_0 decreases rapidly with increasing strain, being less than 20% for strain in excess of 30%. For $\theta_0 = 26°$, 41° and 58°, the curves of θ versus strain and ϕ versus strain for unloaded specimens were not distinguishable from the corresponding curves for loaded specimens. The load applied to a specimen in the straining jig passed through a maximum during the application of the strain increment and then relaxed rapidly while the specimen was held under fixed grip conditions. After about 10 min the remaining relaxation was small so that the SAX exposure, taken over a period of approximately 200 min after the strain application, and the WAX exposure, taken 10 min after the SAX exposure, were taken under an approximately constant stress (Fig. 4). The maximum stress observed during the application of the strain was taken as a measure of the stress at which the deformation mechanisms operated.

4.1. Chain slip and fibrillar slip

Taken together, these accounted for all of the deformation at the two highest angles, $\theta_0 = 41°$ and 58°. This is shown by the variation of θ with strain, which follows the curve predicted for slip processes parallel to the chain direction (Fig. 5). The departure of the value of ϕ from the curve predicted for chain slip alone shows that fibrillar slip occurred (Fig. 6) and became relatively more important at higher strains (Fig. 7), as found by Hinton *et al.* [4]. At $\theta_0 = 26°$ and 8° chain and fibrillar slip occurred along with other deformation mechanisms (Fig. 8), fibrillar slip again becoming more important at higher strains. Over the range of angles $\theta_0 = 8°$ to $\theta_0 = 58°$ the trend was for fibrillar slip to become less important relative to chain slip at a given strain as the angle θ_0 increased. The stress measurements showed that chain slip could occur at a shear stress, resolved in the chain direction, of as little as 9 MNm^{-2}.

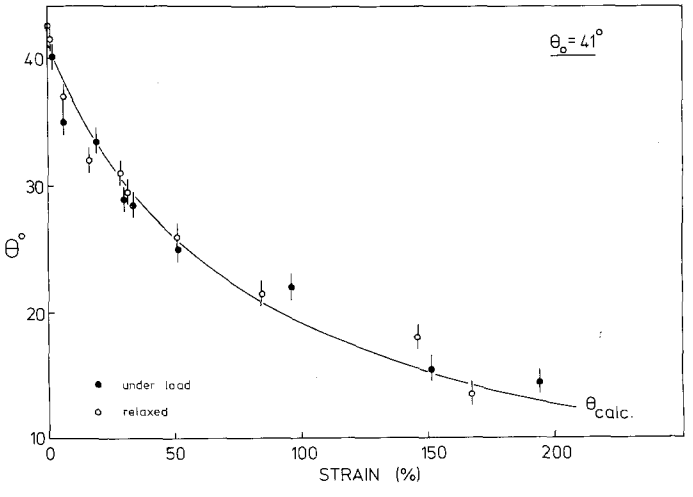

Figure 5 Variation of *c*-axis orientation with strain, $\theta_0 = 41°$. Full line indicates variation of θ predicted for slip parallel to chain direction.

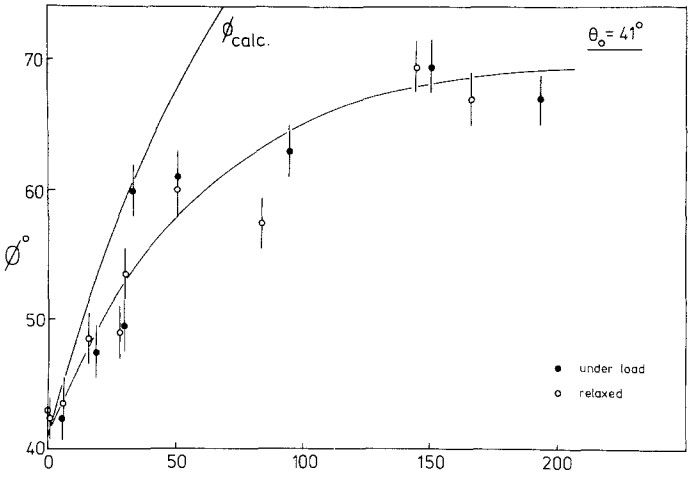

Figure 6 Variation of lamellar normal orientation with strain, $\theta_0 = 41°$. Heavy line (ϕ_{calc}) indicates variation of ϕ predicted for chain slip as sole mechanism.

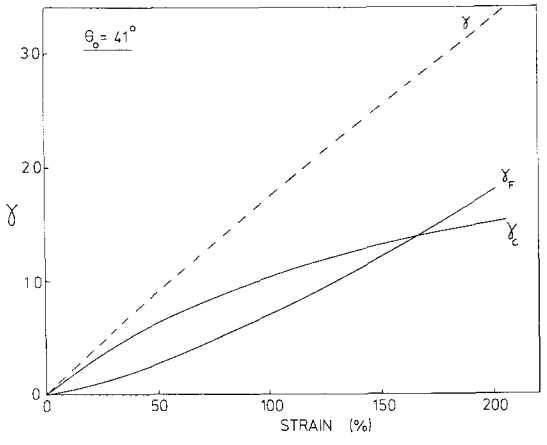

Figure 7 Components of the shear strain due to fibrillar (γ_F) and chain (γ_C) slip, $\theta_0 = 41°$.

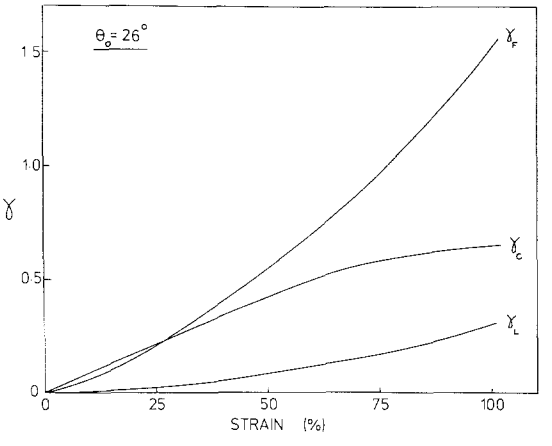

Figure 8 Components of the shear strain due to fibrillar (γ_F), chain (γ_C) and lamellar (γ_L) slip, $\theta_0 = 26°$.

4.2. Lamellar slip

This mechanism was observed only at $\theta_0 = 8°$ and 26° as a relatively minor component of the deformation (Fig. 8). This is in contrast with the results of Pope and Keller [5] on double texture HDPE; however, the orientation of lamellae relative to the chain direction is more favourable for lamellar slip in double texture samples than in the single crystal texture samples used in this work. At $\theta_0 = 8°$ evidence for a small amount of reversible lamellar slip was obtained in that θ values under load were significantly larger than θ values after unloading (Fig. 9). This result is similar to that of Young *et al.* [2] who found reversible lamellar slip in HDPE in compression at $\theta_0 = 16°$. However at $\theta_0 = 26°$ there was clear evidence of permanent lamellar slip in the departure of the observed values in both loaded and unloaded specimens from those predicted by chain and fibrillar slip alone (Fig. 10). The fact that lamellar slip was observed only at smaller values of θ_0 can be understood on considering the observed values of the shear stress resolved onto the lamellar plane (Fig. 11). The fact that lamellar slip was not observed at $\theta_0 = 41°$ indicates that the stress required to initiate permanent lamellar slip is approximately $50\,MNm^{-2}$. It is worth noting also that the effect of chain slip is to bring the lamellae into a more favourable orientation for lamellar slip at lower values of θ_0 and into a less favourable one at higher values of θ_0.

4.3. Lamellar separation

A decrease in the spacing of the small angle maxima indicated lamellar separation at $\theta_0 = 0°$ 8° and 26°. In the case of $\theta_0 = 0°$ an anomaly

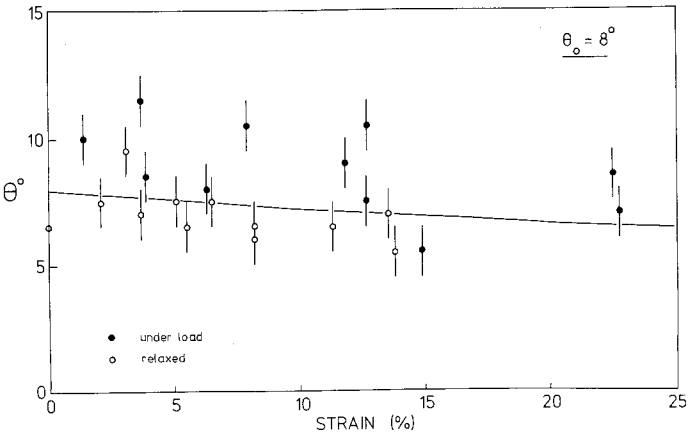

Figure 9 Variation of *c*-axis orientation with strain, $\theta_0 = 8°$. Full line indicates predicted variation of θ for slip in the chain direction.

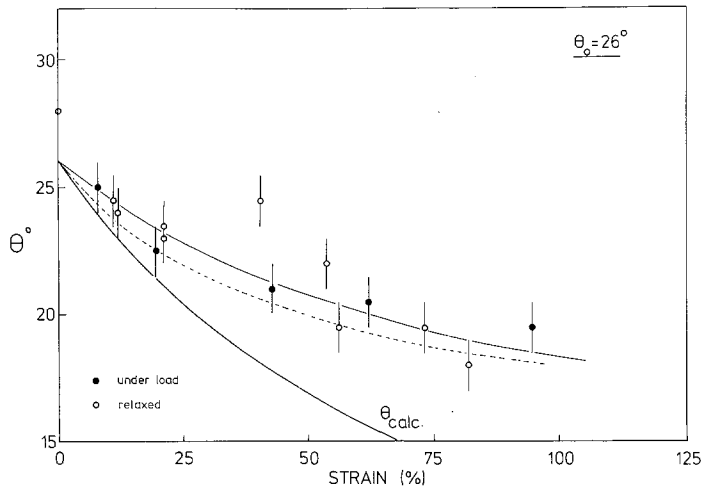

Figure 10 Variation of *c*-axis orientation with strain, $\theta_0 = 26°$. Heavy line (θ_{calc}) indicates predicted θ variation for slip in the chain direction. Dashed line (– – –) indicates shift of experimental data after allowance for strain component due to lamellar separation.

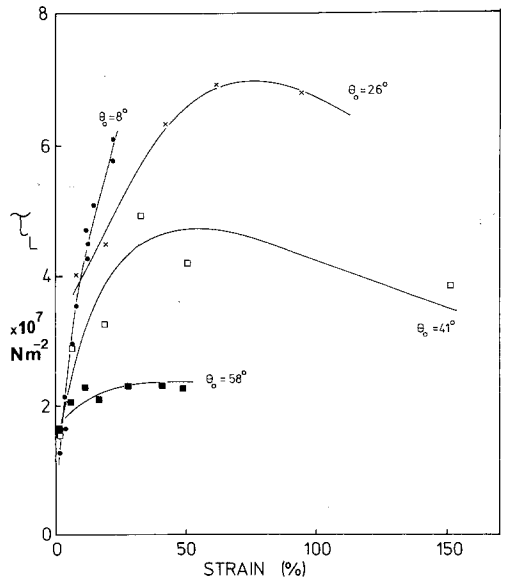

Figure 11 Variation of shear stress τ_L resolved on to lamellar plane as a function of strain for samples with $\theta_0 = 8°, 26°, 41°$ and $58°$.

arose in that the apparent value of the lamellar separation strain $\delta d/d$ derived from the positions of the maxima on the SAX pattern was higher than the applied strain e (Fig. 12). An anomaly of this type has been previously reported for HDPE by Yamada *et al.* [10], but without explanation. In our case the anomaly can probably be attributed to the addition to the lamellar scattering maxima of the tail of the strong central scattering which develops during straining at $\theta_0 = 0°$; the central scattering is believed to be due to voids. This can cause a shift of the positions of the maxima to smaller angles. Inhomogeneity of strain, suggested by Pope and Keller [5] as an explanation of a similar anomaly in low-density polyethylene which does not show voiding, may also play a part. It may be noted that, if interlamellar separation decreases the density of the interlamellar phase, as would be expected, then regions having a high interlamellar separation will contribute a higher intensity to the SAX pattern through the greater density difference between

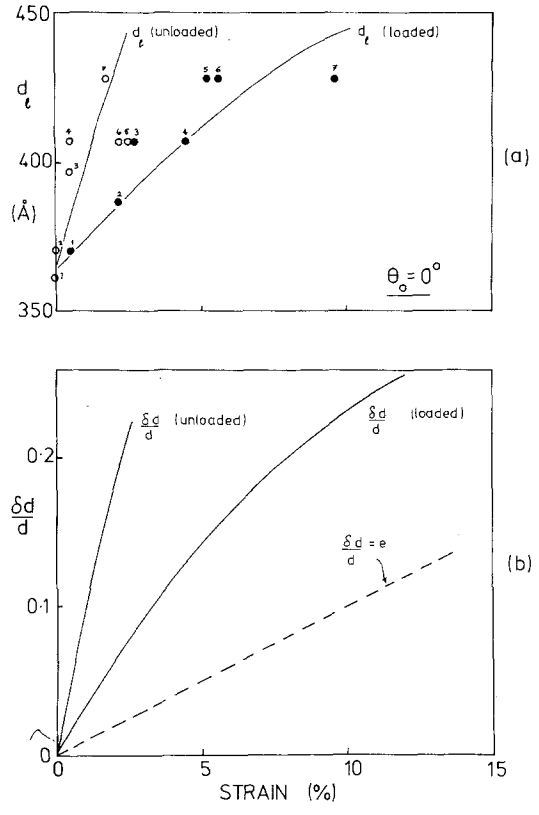

Figure 12 (a) Lamellar spacing d_l as function of strain, $\theta_0 = 0°$. (•) spacing under load; (○) spacing after unloading. (b) Lamellar separation strain $\delta d/d$ as function of strain, $\theta_0 = 0°$.

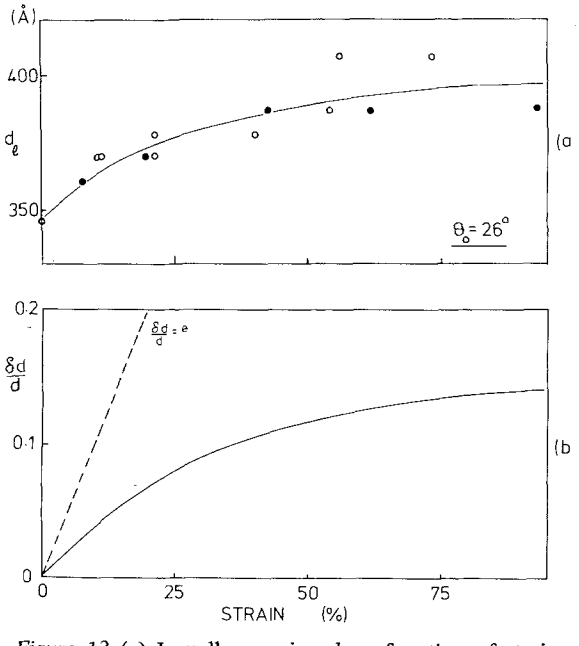

Figure 13 (a) Lamellar spacing d_l as function of strain, $\theta_0 = 26°$. (•) under load; (○) after unloading; (b) Lamellar separation strain $\delta d/d$ as function of strain, $\theta_0 = 26°$.

lamellar and interlamellar material in such regions. At $\theta_0 = 0°$ the greater part of the imposed strain is recovered on unloading but the apparent interlamellar separation is not recovered (Fig. 12). This may be attributed to the fact that voiding remains after unloading and also perhaps that in some regions of high interlamellar separation the limit of reversibility is reached.

At $\theta_0 = 8°$ and $\theta_0 = 26°$ where voiding is much less marked, the values of $\delta d/d$ were less than the macroscopic strain and may be interpreted with more confidence. At $\theta_0 = 8°$, $\delta d/d$ represented approximately half the imposed strain but at $\theta_0 = 26°$ $\delta d/d$ was not simply proportional to the imposed strain and became a relatively minor component at high strains (Fig. 13). The stress measurements indicate that a stress component normal to the lamellae of approximately 60 MNm^{-2} is required to initiate permanent lamellar separation.

4.4. Martensitic transformation

Although the plane strain nature of the deformation shows that stress-induced martensitic transformation cannot account for an important fraction of the strain, the transformation was observed to have occurred at high strains in all but the $\theta_0 = 0°$ and 8° specimens. The transformation appeared to be partly reversible, the intensity of the (0 0 1) monoclinic reflections decreasing upon unloading. For $\theta_0 = 26°$ the monoclinic reflections appeared only after a strain of 40% and remained very weak. At $\theta_0 = 58°$ the monoclinic (0 0 1) reflections appeared at 10% strain and increased in intensity with increasing strain until at 100% strain it was comparable in intensity to the orthorhombic (2 0 0) which has a similar structure factor. This suggests that a substantial fraction of the material had transformed. The orientation distribution was found to be not sharp enough to allow the mode of the transformation to be determined. Previously determined modes for HDPE are the 1_1 and 1_2 modes for which the shape shear strain is 0.201 [6, 7]. The orientation factors for these modes are in our case relatively unfavourable so that for $\theta = 41°$ for example the shear strain must be multiplied by factor of 0.09 and 0.1 for the 1_1 and 1_2 modes respectively, to give the resultant tensile strain. In these cases the transformation of the entire specimen would yield a tensile strain of the order of only 2%. Although the contribution of the martensitic transformation

to the total strain is believed to be negligible it does occur at a relatively low stress level. Thus it was observed when the stress component normal to the chain direction was as low as $15\,MNm^{-2}$. Without knowing the mode of the transformation the appropriate resolved shear stress is not known but it must be less than or equal to $7.5\,MNm^{-2}$, and is therefore of the same order of magnitude as the resolved shear stress for chain slip. Young and Bowden [6] also found that the resolved shear stresses for martensitic transformation and chain slip were the same within experimental error in their studies on the compressive behaviour of single crystal texture HDPE samples.

5. Summary and conclusions

The mechanism of tensile deformation observed in oriented HDPE at room temperature has been found to vary with the orientation of the tensile axis. The most generally important mechanisms are chain slip and fibrillar slip, occurring at all orientations other than $\theta_0 = 0°$ and carrying all the measured strain at higher values of θ_0 ($= 41°$ and $58°$). The relative importance of fibrillar slip to chain slip increases at higher strains and at lower values of θ_0. Mechanisms involving preferential deformation of the interlamellar phase, lamellar slip and lamellar separation, occur only at smaller values of θ_0 ($8°$ and $26°$ for lamellar slip; $0°$, $8°$ and $26°$ for lamellar separation). The stresses required for these processes are relatively high; a resolved shear stress of $50\,MNm^{-2}$ for lamellar slip as opposed to $9\,MNm^{-2}$ for chain slip for example. The martensitic transformation is observed at higher strains for higher values of θ_0 ($26°$, $41°$, $58°$) but does not carry a significant proportion of the total applied strain.

References

1. P. B. BOWDEN and R. J. YOUNG, *J. Mater. Sci.* 9 (1974) 2034.
2. R. J. YOUNG, P. B. BOWDEN, J. M. RITCHIE and J. G. RIDER, *ibid.* 8 (1973) 23.
3. D. M. SHINOZAKI and G. W. GROVES, *ibid.* 8 (1973) 1012.
4. T. HINTON, J. G. RIDER, and L. A. SIMPSON, *ibid.* 9 (1974) 1331.
5. D. H. POPE and A. KELLER, *J. Polymer Sci. (Phys).* 13 (1975) 533.
6. R. J. YOUNG and P. B. BOWDEN, *Phil. Mag.* 29 (1974) 1061.
7. P. ALLAN, E. B. CRELLIN and M. BEVIS, *ibid.* 27 (1973) 127.
8. R. W. GRAY and R. J. YOUNG, *J. Mater. Sci.* 9 (1974) 521.
9. S. G. BURNAY, *D. Phil. Thesis,* Oxford 1976.
10. M. YAMADA, K. MUJASKA and K. ISHIKAWA, *J. Polymer Sci. A2* 9 (1971) 1083.

Received 10 June and accepted 11 July 1977.